

# Electronic polarization of BN nanotubes: A first-principles study of the chirality dependence

Tomoya Ono, Jun Otsuka, and Kikuji Hirose

*Department of Precision Science and Technology,*

*Osaka University, Suita, Osaka 565-0871, Japan*

(Dated: February 6, 2019)

## Abstract

A first-principles study of the electronic polarization of BN nanotubes and a BN graphitic sheet under an external electric field has been performed. We found that the polarization of zigzag nanotubes increases with decreasing diameter while that of armchair nanotubes decreases. When the atomic geometry of the nanotubes is optimized, the polarizations of both types of nanotubes are suppressed. The variation of the polarization is closely related to the exterior angle of the BN bonds around the B atoms. The increase in the polarization of the zigzag nanotubes with decreasing diameter is caused by the large variation of the exterior angle when they are wrapped into the tubular form. On the other hand, the decrease in the BN bond length results in the weak polarization of thin armchair nanotubes.

PACS numbers: 73.22.-f, 77.22.Ej

## I. INTRODUCTION

Since the discovery of carbon nanotubes (C-NTs)[1], many experimental and theoretical studies have focused on synthesizing nanometer-scale tubular forms of various materials and revealing their properties. III-V semiconductors have also attracted considerable attention due to their many potential applications in high-power and high-temperature devices, because the properties of bulk BN are similar to those of diamond, for example, excellent thermal conductivity, high chemical resistance, and high melting point. In addition, since BN is a piezoelectric material, its tubular structure is a candidate for applications in nanometer-scale sensors and actuators. It has so far been reported that single-walled BN nanotubes (BN-NTs) can be produced by arc discharge[2] and chemical substitution reactions[3]. On the theoretical side, there have been several studies on the polarization of C-NTs and BN-NTs[4, 5, 6, 7, 8, 9, 10]. For example, Kozinsky and Marzari[9] reported that the longitudinal polarizability of single-wall C-NTs varies as the inverse square of the band gap, while the transverse polarizability is proportional to the square of the effective radius. Chen *et al.*[11] proved that a gradual reduction of the band gap of BN-NTs occurs because of the larger ionicity of the BN bond. However, there still remains much to be learned about the electronic polarization of the NTs composed of III-V elements.

In this paper, we carry out a first-principles calculation on the longitudinal electronic polarization of BN-NTs using the Berry phase approach[12, 13]. When a BN graphitic sheet is simply wrapped into a zigzag tubular form, the longitudinal electronic polarization of the NT increases as the diameter decreases. On the other hand, the polarization of armchair NTs decreases with decreasing diameter, which cannot be explained by the conventional interpretation of the relationship between the energy band gap and the polarization[14], because the band gap of the graphitic BN sheet is larger than that of the BN-NTs. When the atomic geometries of the NTs are relaxed by first-principles structural optimization, the BN bonds buckle, which suppresses the polarization. The characteristics of the BN bond around B atoms have a larger effect on the polarization than those of the bond around N atoms.

The rest of this paper is organized as follows. In Sec. II, we briefly describe the method used in this study. Our results are presented and discussed in Sec. III. We summarize our findings in Sec. IV.

## II. COMPUTATIONAL METHODS

Figure 1 shows the computational models of the BN-NTs and the graphitic BN sheet. The BN bond length  $a_0$  is set to 1.43 Å, which is reported by Guo and Lin[8]. The calculations are performed within the local density approximation[15] of density functional theory[16, 17] using the real-space finite-difference approach[18, 19, 20] and the norm-conserving pseudopotentials of Troullier and Martins in the Kleinman-Bylander representation[21, 22, 23]. The cutoff energy is set to 110 Ry, which corresponds to a grid spacing of 0.30 a.u., and a higher cutoff energy is taken to be 987 Ry in the vicinity of the nuclei with the augmentation of double-grid points[19, 20]. The periodic boundary condition is imposed on the supercell in all directions. During the first-principles structural optimization, we relaxed all the atoms using a conjugate gradient algorithm. In the case of the NTs, four layers of atoms along the tube axis are contained within a vacuum region (more than 10 Å) between NTs in the neighboring supercells. The integration over the Brillouin zone for the tube axis is performed by the equidistant sampling of 10 (18)  $k$ -points for the zigzag (armchair) NTs. In the case of the graphitic sheet, the supercell is  $3a_0 \times \sqrt{3}a_0 \times L_z$ , where  $L_z$  is the length of the supercell along the  $z$  axis, which is taken to be 20 Å to avoid the interaction between the adjacent sheet. The sampling  $\mathbf{k}$ -points over the Brillouin zone is  $10 \times 18 \times 1$ . We have ensured that the enlargement of the supercell and the increase of the number of the sampling  $\mathbf{k}$  points do not change our conclusions significantly.

An electric field of 0.1 V/Å is applied along the NT axis and along the directions parallel to the graphitic sheet. The electronic ground state and the optimized electronic structures under external electric fields are determined using the discrete Berry phase scheme proposed by Umari and Pasquarello[13]. The electronic polarization can be expressed as

$$\mathbf{P} = -2e \sum_i \langle \mathbf{r}_i \rangle, \quad (1)$$

where  $i$  is the band index,  $-e$  is the electron charge, the factor 2 indicates the spin freedom, and  $\langle \mathbf{r}_i \rangle$  is the center of the density distribution of the occupied wave functions  $\psi_i$ , and is defined by the following formula[13]:

$$\langle \mathbf{r}_i \rangle = -\frac{L}{2\pi} \Im \ln \left\langle \psi_i | e^{-i\frac{2\pi}{L}\mathbf{r}} | \psi_i \right\rangle, \quad (2)$$

with  $L$  being the length of the supercell. The variation of the polarization due to the external

electric field is defined by  $\Delta\mathbf{P}^E = \mathbf{P}^E - \mathbf{P}^0$ , where  $\mathbf{P}^E$  ( $\mathbf{P}^0$ ) corresponds to the electronic polarization when the external electric field  $E$  is present (absent).

### III. RESULTS AND DISCUSSION

Figure 2 shows the electronic polarization of the NTs and the graphitic sheet. Although the graphitic sheet is not symmetric with respect to the  $xy$  rotation as well as the  $yz$  plane, the polarizations of these directions (0.0362 a.u./atom) are comparable. The contributions of the  $\pi$  and  $\sigma$  electrons to the polarization are 0.0234 a.u./atom and 0.0042 a.u./atom, respectively. The electronic polarization under the external electric field as a function of the diameter of the BN-NTs without the structural optimization (unrelaxed BN-NTs) is plotted by broken lines in Fig. 2. The polarization of the zigzag NTs increases as their diameters become small. In contrast, the armchair NTs exhibit the opposite tendency upon polarization; the electronic polarization of the armchair NTs becomes smaller than that of the graphitic sheet and decreases as the NTs become thin. When the atomic geometries of the BN-NTs are fully relaxed (relaxed BN-NTs), the B atoms move toward the central axis of the NTs, and the N atoms move in the opposite direction. The BN bond configuration around the B atoms becomes planar. The radial buckling is 0.047 Å for the (5,5) NT and 0.051 Å for the (9,0) NT. The total electronic polarization is plotted by solid lines in Fig. 2. For both chiralities, the total electronic polarization of BN-NTs is suppressed. Although the different polarization tendency of the relaxed NTs was found in the previous first-principles study[10], the origin of the interesting polarization is still unsettled question. It is reported that the electronic polarization of conventional III-V compounds increases with the reduction of the band gap[10, 14]. In addition, all BN-NTs are semiconductors and their band gap grows monotonically with increasing diameter[11]. Our results regarding the armchair NTs are inconsistent with those predicted from these previous studies because the band gap of a BN graphitic sheet is larger than that of BN-NTs.

To discuss the different tendency of the polarization between the zigzag and armchair NTs in detail, we examine the polarization with respect to the BN bond angle and the cross section of the BN graphitic sheet, which varies during the wrapping of the sheet into the tubular form. We first calculate the electronic polarization of the graphitic sheet in which B or N atoms are displaced along the direction perpendicular to the graphitic sheet with the BN

bond length being kept at  $a_0$ . Schematic illustrations of the computational models are shown in Fig. 3, where the neighboring B(N) atoms are alternately shifted toward the positive and negative  $z$  direction. Figure 4 shows the polarization as a function of the exterior angle  $\theta$  of the BN bonds. The polarization increases (decreases) nearly quadratically with the exterior angle around the B(N) atoms, and the variation of the exterior angle around the B atoms has a stronger effect on the increase in the polarization than that around the N atoms. Thus, the polarization becomes stronger as the exterior angle increases. These findings agree with the result that the planar bond configuration around the B atom suppresses the polarization in the case of the relaxed NTs.

We next explore the polarization properties with respect to the BN bond length. The electronic polarization of the graphitic sheet as a function of the ratio of the cross section of the sheets,  $S/S_0$ , is shown in Fig. 5. Here,  $S = tL_{x(y)}$ ,  $t$  is the effective thickness of the sheet[24], and  $L_{x(y)}$  is the length of the supercell in the  $x(y)$  direction. In addition,  $S_0$  is the cross section of the sheet in which the lengths of all the BN bonds are  $a_0$ . The length of the supercell in the direction perpendicular to the external electric field is varied, while that in the direction parallel to the field is fixed and the graphitic sheet is kept flat. For both directions of the external electric field, the polarization proportionally becomes large with increasing lateral length  $L_{x(y)}$ . To explore the relation between the polarizability and the geometrical deformation due to the wrapping into the tubular form, we plot in Fig. 6 the variations of the exterior angle of the BN bonds and the cross section of the BN-NTs as a function of the diameter. When the BN graphitic sheet is wrapped into the tubular form, the exterior angle increases and the cross section becomes small with the decrease in the diameter. The exterior angle of the zigzag NTs varies more than that of the armchair NTs; the large variation of the exterior angle increases the polarization of the zigzag NTs. In contrast, the decrease in the cross section results in the weak polarization of thin armchair NTs.

#### IV. CONCLUSION

We have studied the electronic polarization of BN-NTs and a BN graphitic sheet under finite external electric fields from first principles. We found that the electronic polarization of the zigzag NTs increases as their diameter decreases. On the contrary, the polarization

of the armchair NTs decreases as the NTs become thin. The buckling due to the structural optimization suppresses the polarization of the NTs. The variation of the polarization with the diameter is associated with specific features of the BN bond arrangement, such as the bond angles around the B atoms and the BN bond length. Since this polarization dependence on the chirality is also observed in the case of AlN-NTs, our results indicate the possibility of tuning the dielectric property of III-V NTs by controlling their diameter and chirality.

### Acknowledgements

This research was partially supported by a Grant-in-Aid for the 21st Century COE “Center for Atomistic Fabrication Technology”, by a Grant-in-Aid for Scientific Research in Priority Areas “Development of New Quantum Simulators and Quantum Design” (Grant No. 17064012), and also by a Grant-in-Aid for Young Scientists (B) (Grant No. 17710074) from the Ministry of Education, Culture, Sports, Science and Technology. The numerical calculation was carried out using the computer facilities at the Institute for Solid State Physics at the University of Tokyo, the Research Center for Computational Science at the National Institute of Natural Science, and the Information Synergy Center at Tohoku University.

- 
- [1] S. Iijima, *Nature* (London) **354**, 56 (1991).
  - [2] J. Cumings and A. Zettl, *Chem. Phys. Lett.* **316**, 211 (2000).
  - [3] D. Golberg, Y. Bando, W. Han, K. Kurashima, and T. Sato, *Chem. Phys. Lett.* **308**, 337 (1999).
  - [4] L.X. Benedict, S.G. Louie, and M.L. Cohen, *Phys. Rev. B* **52**, 8541 (1995).
  - [5] D.S. Novikov and L.S. Levitov, *Phys. Rev. Lett.* **96**, 036402 (2006).
  - [6] Y. Li, S.V. Rotkin, and U. Ravaioli, *Nano Lett.* **3**, 183 (2003).
  - [7] E.N. Brothers, K.N. Kudin, G.E. Scuseria, and C.W. Bauschlicher, *Phys. Rev. B* **72**, 033402 (2005).
  - [8] G.Y. Guo and J.C. Lin, *Phys. Rev. B* **71**, 165402 (2005).
  - [9] B. Kozinsky and N. Marzari, *Phys. Rev. Lett.* **96**, 166801 (2006).
  - [10] G.Y. Guo, S. Ishibashi, T. Tamura and K. Terakura, *Phys. Rev. B* **75**, 245403 (2007).

- [11] C.W. Chen, M.H. Lee, and S.J. Clark, *Nanotechnology* **15**, 1837 (2004).
- [12] R. Resta, *Rev. Mod. Phys.* **66**, 899 (1994).
- [13] P. Umari and A. Pasquarello, *Phys. Rev. Lett.* **89**, 157602 (2002).
- [14] N.E. Christensen and I. Gorczyca, *Phys. Rev. B* **50**, 4397 (1994).
- [15] J.P. Perdew and A. Zunger, *Phys. Rev. B* **23**, 5048 (1981).
- [16] P. Hohenberg and W. Kohn, *Phys. Rev.* **136**, B864 (1964).
- [17] W. Kohn and L.J. Sham, *Phys. Rev.* **140**, A1133 (1965).
- [18] J.R. Chelikowsky, N. Troullier, and Y. Saad, *Phys. Rev. Lett.* **72**, 1240 (1994); J.R. Chelikowsky, N. Troullier, K. Wu, and Y. Saad, *Phys. Rev. B* **50**, 11355 (1994).
- [19] K. Hirose, T. Ono, Y. Fujimoto, and S. Tsukamoto, *First-Principles Calculations in Real-Space Formalism, Electronic Configurations and Transport Properties of Nanostructures* (Imperial College Press, London, 2005).
- [20] T. Ono and K. Hirose, *Phys. Rev. Lett.* **82**, 5016 (1999); *Phys. Rev. B* **72**, 085105 (2005); *ibid.* **72**, 085115 (2005).
- [21] L. Kleinman and D.M. Bylander, *Phys. Rev. Lett.* **48**, 1425 (1982).
- [22] N. Troullier and J.L. Martins, *Phys. Rev. B* **43**, 1993 (1991).
- [23] We used the norm-conserving pseudopotentials NCPS97 constructed by K. Kobayashi. See K. Kobayashi, *Comput. Mater. Sci.* **14**, 72 (1999).
- [24] The effective thickness  $t$  can be taken to be arbitrary because it is canceled in  $(S - S_0)/S_0$ .

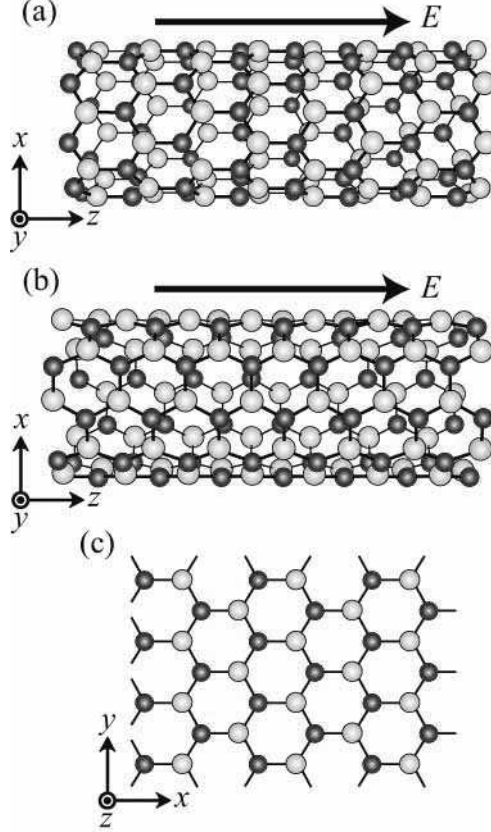


FIG. 1: Computational models of (a) zigzag NT, (b) armchair NT, and (c) graphitic sheet. Light and dark spheres indicate B and N atoms, respectively.  $E$  is an external electric field.

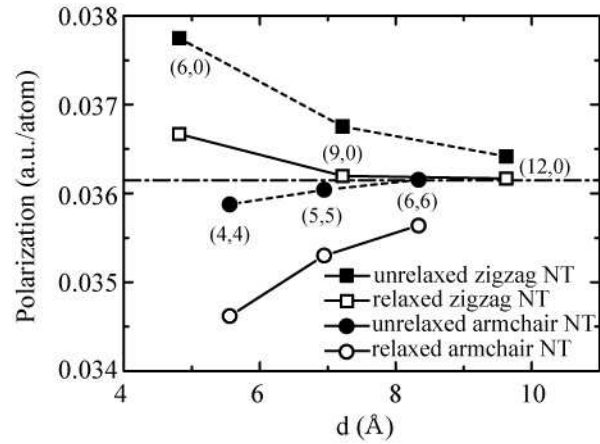


FIG. 2: Electronic polarization of BN-NTs per atom as a function of diameter. The dot-dashed line represents the polarization of the graphitic sheet.

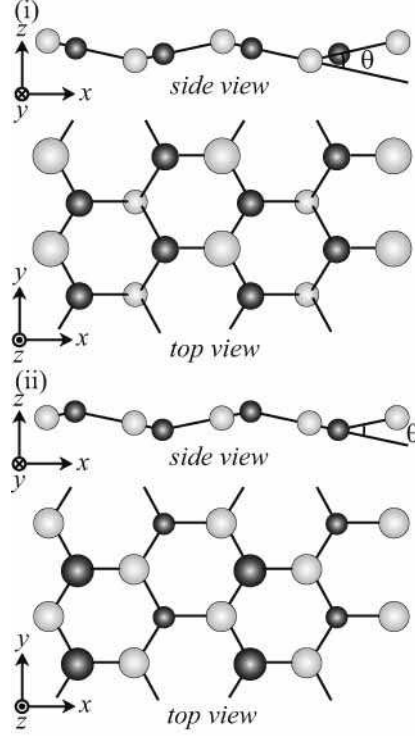


FIG. 3: Computational models of graphitic sheet in which B or N atoms are displaced along the direction perpendicular to the graphitic sheet. (i) B atoms are shifted, (ii) N atoms are shifted. Gray and dark-blue spheres indicate B and N atoms, respectively. In the top views, B(N) atoms are denoted by larger and smaller spheres according to their distance from N(B) atoms.

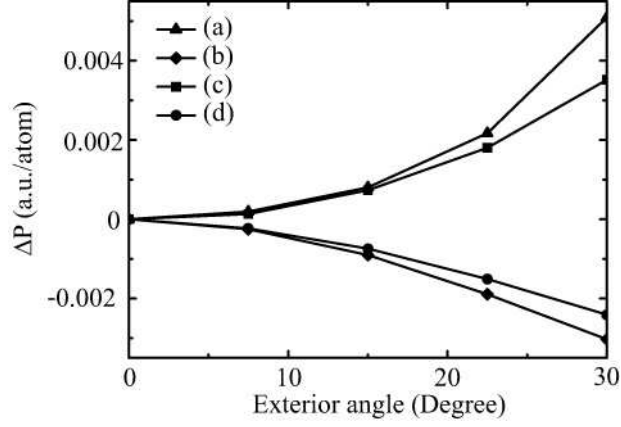


FIG. 4: Variation of electronic polarization,  $\Delta\mathbf{P} = \mathbf{P}(\theta) - \mathbf{P}(0)$ , of BN graphitic sheet as a function of exterior angle  $\theta$  in Fig. 3. (a) and (b) The external electric field is applied along the  $x$  direction. (c) and (d) The external electric field is applied along the  $y$  direction. The curves (a) and (c)[(b) and (d)] show the polarizations of model (i)[(ii)] in Fig. 3.

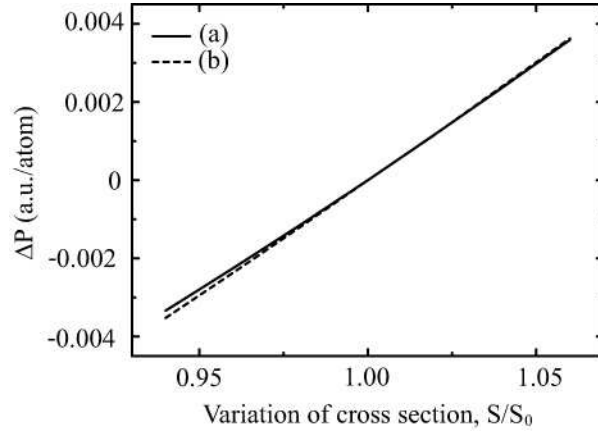


FIG. 5: Variation of electronic polarization,  $\Delta\mathbf{P} = \mathbf{P}(S) - \mathbf{P}(S_0)$ , of BN graphitic sheet as a function of variation of cross section. The computational model is the same as that in Fig. 1 (c). The curve (a)[(b)] shows the polarization of the case that the external electric field is applied along the  $x$ [ $y$ ] direction and the length of the supercell in the  $y$ [ $x$ ] direction is varied.

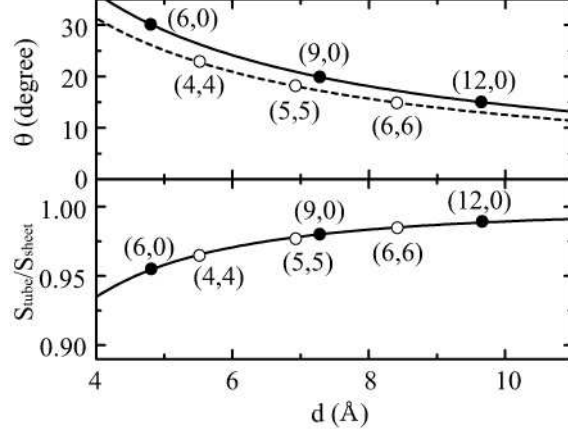


FIG. 6: Variations of exterior angle of the BN bonds and cross section of the BN-NTs as a function of diameter of NTs. The solid and dotted curves are the variations of the zigzag and armchair NTs, respectively.